Macromolecular Nanotechnology

Making nanofibres of mucoadhesive polymer blends for vaginal therapies

Francis Brako [a,b], Bahijja Raimi-Abraham [b], Suntharavathanan Mahalingam [a], Duncan Q.M. Craig [b], Mohan Edirisinghe [a,*]

[a] Department of Mechanical Engineering, University College London, Torrington Place, London WC1E 7JE, UK
[b] University College London, School of Pharmacy, 29-39 Brunswick Square, London WC1N 1AX, UK

ARTICLE INFO

ABSTRACT

Nanofibres from mucoadhesive polymers could combine their material properties with unique structural characteristics for superior drug delivery performance. However, due to their chain structure a significant proportion of mucoadhesive polymers such as polysaccharides cannot be easily spun into fibres. In this study, we demonstrate the possibility of using polymer blends for the preparation of nanofibres that offer substantial mucoadhesive capabilities. Fibres from four different polymers were obtained by pressurised gyration at different working pressures and a rotation speed of 24,000 rpm. Electron microscopy indicates that structurally well-defined fibres with diameters from less than 100 nm upwards were successfully produced. Quantitative relationships between the physical properties and fibre characteristics were established while the fibre compositions were confirmed to contain features likely to confer mucoadhesive properties. Finally, a combination of texture analysis and atomic force microscopy was used to verify the benefit of transforming polymer powders into nanofibre structures, as far as mucoadhesive potential is concerned.
© 2015 The Authors. Published by Elsevier Ltd. This is an open access article under the CC BY license (http://creativecommons.org/licenses/by/4.0/).

1. Introduction

The increasing utility of nanofibres within diverse fields including tissue engineering, drug delivery, filtration, conducting composites, photonics and fuel cells is becoming increasingly prominent [1–3]. For example, it has been shown that extremely light nanofibre layers (around 0.05–0.1 g over a square meter area) offer excellent filtration properties, as well as possessing the ability to support the growth of human, animal and bacteria cells, thereby offering application for decontamination technologies and tissue engineering [4].

Nanofibres have large surface area, specifically characterised by a high surface-to-volume ratio and such fibres can contain significant porosity defined by a relatively small pore size [5,6]. This benefit is even clearer when illustrated quantitatively, taking their cylindrical surface into consideration. For instance a fabric made with fibres of diameter 10 nm will have a surface area in the region of 350 m^2/g compared to only 0.35 m^2/g for the same size made of 10 μm fibres. Although higher surface areas are achievable with some nanoporous granules and powders, nanofibre units are easier handled and manipulated than powders [7]. The easier manipulation of nanofibres means they could be better adapted to fit the requirements of

an effective and safe drug delivery system. An area of drug delivery where the properties of nanofibres could be valuable is topical/mucosa delivery aided by adhesion, an example being the vaginal route of administration.

Notwithstanding these prospects, the availability of adequate quantities of nanofibre structures have been a drawback, in that there remains a considerable gap between demand and supply [8]. Some drug encapsulation in biodegradable nanofibres have been attempted in the past, though mainly by electrospinning [9–11]. Electrospinning however has many associated limitations including cost from high voltage usage and the relatively low yield, even over long periods of spinning [12,13]. A newly invented pressurised gyration system for producing nanofibres [14] offers fresh prospects for producing nanofibre. Pressurised gyration offers a flexible processing environment which can be manipulated to produce structures fit for function and purpose.

The objective of this work was to identify and analyse the various conditions required for optimal production of mucoadhesive nanofibres utilising blends of polymers with different adhesive profiles. Fibres obtained were intended to serve as the basic unit for design of a drug delivery system to be applied to mucosa surfaces. Studies here ranged from assessment of the feed solutions through to nanofibre and performance characterisation in order to correlate composition, manufacture and efficacy.

In terms of performance, the main thrust of this study was to examine the possibility of achieving mucoadhesion for drug delivery via contact with a hydrated biological surface. In order to assess this outcome, it was necessary to develop a model for quantitatively comparing adhesion functions among the batches of fibres produced that may correlate to adhesion to a mucosal environment. While several methodologies are available [15], this work is among the earliest in the area of assessing the mucoadhesive properties of nanofibres, and hence some modifications to the conventional method of assessing mucoadhesive strengths was adopted.

A wide range of materials have been explored for fabrication into nanofibres [16–18], while similarly there are now a range of well-recognized pharmaceutically acceptable polymers with mucoadhesive properties [19–23]. However, there is a paucity of work exploring the combination of mucoadhesion and nanofibre formation, an area which this study aims to address in the context of the pH (4 ± 0.5) and hydration environment of the vagina [20]. Furthermore, several mucoadhesive polymers have not been explored extensively for fibre formation. Here we examine the fibre-forming and mucoadhesive properties of carboxymethylcellulose (CMC), sodium alginate (NaAlg), polyacrylic acid (PAA) and polyethyleneoxide (PEO), all of which are recognized mucoadhesives. PEO is also used as a spinning agent to enable the other materials to be easily spun into fibres. In this work, these materials have been studied individually and in combination so as to identify the most suitable materials from the viewpoint of both fibre formation and mucoadhesive performance. More information on these materials is given in Supplementary Information.

2. Experimental details

2.1. Materials

Sodium carboxymethylcellulose (CMC), average M_w ~250,000, polyethyleneoxide (PEO) average M_w ~200,000, polyacrylic acid (PAA), M_w 450,000 and medium viscosity sodium alginate (SA), were obtained from Sigma–Aldrich Company Ltd, Gillingham, UK. All polymers were used without further purification. The solvent used throughout was purified water, freshly distilled. Sodium chloride, potassium chloride, calcium hydroxide, lactic acid, glycerol, urea, glucose, mucin from porcine stomach and bovine serum albumin obtained from Sigma–Aldrich Company Ltd, Gillingham, UK were all of analytical grade and used without further purification to prepare the simulated vaginal fluid used throughout the mucoadhesive studies [24].

2.2. Methods

2.2.1. Polymers solution preparation and characterisation

Uniform solutions of polyethyleneoxide, carboxymethylcellulose, polyacrylic acid and sodium alginate were obtained by continuous magnetic stirring followed by sonication for 10 min using a Branson Sonifier 250 (Danbury, Connecticut, USA). The viscosity for each polymer solution or blend was measured using a Brookfield DV-111 viscometer (Harlow, Essex, UK) at a shear stress of 3.5 Pa. Surface tension was measured by plate method using a Kruss K9 tensiometer (Hamburg, Germany). In each type of characterisation, five separate measurements were taken and their means used for further analyses.

2.2.2. Fibre spinning

The novel technique of pressurized gyration [14] was used to spin out the fibres at ambient temperature (25 °C). In brief, this consists of a rotating perforated drum which is spun under pressure so as to extrude streams of polymer solution, with the solvent being evaporated during flight to yield fibres at high volume and uniformity. 3 ml of solution was placed in the aluminium vessel and spun at a rotational speed of 24,000 rpm and working pressure of 0.1, 0.15 and 0.2 MPa as stated. Samples were obtained manually by simply collecting the ejected fibres.

2.2.3. Microscopy

Samples from each batch of fibres were analysed by scanning electron microscopy (SEM), JEOL JSM 630 IF (Tokyo, Japan), for assessment of morphology and size distribution of the fibres, the latter generated from studying 100 fibres. Samples were mounted on SEM stubs with the aid of two-sided adhesive carbon discs obtained from Agar Scientific, Stansted, UK. Each mounted sample of fibres was gold coated for 90 s using Quorum Q150R pumped sputter coaters (Quorum Technologies, Lewes, UK). Coated samples were analysed at an operating voltage of 5 kV. Record of images was produced with the aid of SemAfore software, also provided by the SEM manufacturer.

2.2.4. Spectrophotometry

FTIR analysis was performed via Attenuated Total Reflection Fourier Transform Infrared spectroscopy (ATR-FTIR) measurements (Bruker Vertex 90 spectrometer), and spectrographs were interpreted using OPUS Viewer version 6.5 software. Scans were completed at ambient temperature and at 2 °C intervals between 50 and 80 °C using Specac Golden Gate (Orpington, UK) to study the effect of heat on the samples beyond the melting point of polyethylene, which for this grade is approximately 65 °C. Relative solubilities of nanofibre samples in the simulated mucus environment were determined by measuring the surface roughness of residual films from nanofibre and mucin mixtures using a Bruker Multimode 3 atomic force microscope (Coventry, UK). A film area of 225 μm² was scanned at a rate of 1 Hz using a TESPA-V2 probe (Bruker, Coventry, UK) with a cantilever having a spring constant of 42 N/m. Height images were obtained using the tapping mode. Measurements from images were obtained using ImageJ software (National Institute of Health, Maryland, USA).

2.2.5. Mucoadhesive studies

The extent of interactions between fibres and mucin under simulated conditions similar to a vaginal environment were studied using a Texture analyser, TA-XT2 (Food Technology Corporation, Virginia, USA); the approach used was to measure the breaking properties of mixes of the polymer and simulated mucus [25]. A predetermined force of 20 g (force) was applied by an acrylic probe of cross sectional area 50 mm² for a contact period of 0.1 s. Pre-test speed of probe was 0.5 mm/s while return speed was 0.5 mm/s over a 4 mm distance. The force required to break up polymer/mucin gel by separating the probe from the sample was measured; it was ensured that the breakage occurred within the gel rather than between the gel and probe.

3. Results and discussion

A preliminary investigation to determine a suitable proportion of mucoadhesive polymer to be incorporated in blends and an optimal working pressure was carried out using three blends made up of different proportions of PEO and CMC. Details of the solutions, working conditions and dimensions of resulting fibres are given in Table 1.

3.1. Effect of blend composition on fibre characteristics

As shown in Table 1, blends containing 25 wt% of CMC solution gave nanofibres with lowest average diameter, while batches containing 10 wt% of CMC solution yielded larger sized fibres. These indicate an inverse relationship between amount of CMC in the blends and fibre diameter.

With respect to these blends, because of the extent of interactions between oxygen from ether groups in PEO and hydroxyl groups from the polysaccharide cellulose derivative, CMC significantly affects solution properties and ultimately, the physical properties of resulting fibre. These interactions at the molecular level have been thought to enhance chain entanglement and subsequently fibre formation [26,27]. In effect, fibre formation and possibly its physical characteristics such as size depend on the level of polymer chain entanglement. This is also influenced by extent of interaction which is dependent on the source of reactants, in this case, CMC as that is the constituent being varied. The fibre diameter variation seen in relation to changing amount of CMC in blends can be explained in terms of its role in affecting chain entanglement in the blend.

3.2. Effect of working pressure

It was observed that generally, increasing the working pressure decreased the average fibre diameter. However, this inverse relationship between working pressure and average fibre diameter was seen clearest among batches prepared from

Table 1
Solution and pressure working conditions for fibres generated from blends of PEO and CMC.

Weight ratios of PEO solution: CMC solution (from 15 wt% PEO solution and 4 wt% CMC solution)	Average fibre diameter (nm) ± SD at pressures shown below		
	0.1 MPa	0.15 MPa	0.2 MPa
90:10	266 ± 49	280 ± 48	234 ± 47
86:14	189 ± 23	270 ± 54	192 ± 29
75:25	202 ± 54	194 ± 34	161 ± 37

blends with highest CMC content, 25 wt%. Also, there was a clear reduction in average fibre diameter for all batches when pressure was increased from 0.15 to 0.2 MPa.

These observations strongly points to two possibilities. Firstly, regardless of blend composition, reduction of fibre size by pressure was seen above a working pressure of 0.15 MPa but not necessarily at a lower pressure. Secondly, unlike a solution system made up of single polymer, where increasing working pressure decreases fibre size, regardless of their concentrations [14] systems such as blends of polymers tend to respond to pressure based on the proportions of the constituents. The molecular interactions that occur among the polymers making up the blends seem to influence how pressure affects the outcome of the fibre formation. For instance the batch containing 25 wt% CMC solution showed uniform decrease in fibre size across 0.1, 0.15 and 0.2 MPa pressures whereas those with less CMC content did not respond in this way through increasing pressure.

3.3. Fibres from PEO blends with CMC, Alginate and PAA

The outcome from the preliminary investigations informed the choice of parameters for producing nanofibres from blends with PEO and alginate or polyacrylic acid in addition to those containing CMC. Each 100 ml of polymer blend contained 75 ml of 15 wt% PEO and 25 ml of 4–5 wt% mucoadhesive polymer. This is due to a similar blend composition for PEO and CMC yielding fibres that responded desirably towards changing working pressure. Also a pressure of 0.15 MPa was chosen as the effect of the lower pressure of 0.1 MPa offered no desirable effect on fibre diameter generated. Scanning electron micrographs (Fig. 1) show well-structured nanofibres confirming the possibility of producing these by pressurised gyration. The fibre diameter distributions produced, which are representative of the composition and forming conditions, are polydispersed and the polydispersity index (PI) varied from 15–35%. However, the polydispersity could be tailored to suit. For example, Fig. 1b has PI of 23% and Fig. 1c gives a PI of 15%.

A strong correlation was seen between solution properties and fibre size. As shown in Fig. 2a and b, viscosity and surface tension increased in the order PEO/PAA > PEO/CMC > PEO/Alginate. The exact reverse is seen in the mean diameter of fibres produced, thus establishing the order PEO/PAA < PEO/CMC < PEO/Alginate. The conventional observation in pressurised gyration has been that lower viscosities and surface tension usually result in fibres with smaller diameters and vice versa [14,28]. This was confirmed in the batch containing only PEO which had the lowest viscosity and surface tension (2158 mPa s and 54.9 mN/m respectively), which generated the least average fibre diameter among the batches. However, batches from solutions containing different polymers have consistently shown an inverse relationship between viscosity and surface tension on one side and fibre size on the other. The role of molecular interactions between various polymers making up the blends and their cascading effects explain these inverse relationships. Viscometry analyses of blends have established, based on molecular interaction that systems containing different polymer constituents might show a positive or negative deviation from expected ideal behaviour of those containing a single polymer [29].

3.4. Composition of nanofibres

A combination of FTIR at ambient and elevated temperature was employed to verify the compositional features of batches of nanofibres produced. Though steps were taken to ensure adequate mixing and homogeneous mixing in the blends, it is important to confirm constituents of a nanofibre produced to establish that expected materials are indeed present. Firstly, the extremely high forces from the rotation and pressure applied during fibre formation could result in phase separation, especially in the absence of appreciable molecular interaction between the separate polymers in solution. Experimental and mathematical models have been used to describe the behaviour of polymers blends, including possible separation under certain stress conditions [30]. The rationale for ATR-FTIR was to compare spectra for any peak shift usually associated with molecular interactions among polymers. For instance hydrogen bonding and complexation may occur when polymer blends are formed, resulting in changes in bond energies and frequencies of valence and deformation vibrations [27]. These changes detectable on the FTIR spectra are also helpful in confirming the presence of polymers expected in the nanofibres.

As expected, FTIR spectra of PEO only and blends containing PEO gave profiles similar to those of pure PEO. This is because significant proportions of all blends are PEO. A peak at 843 cm^{-1} indicating $-CH_2-CO$ rocking/stretching is typical for PEO (Fig. 3a). Furthermore, spectra of the various blends showed peaks typical of constituent materials other than the PEO. For instance the blend containing alginate showed an additional peak at 1613 cm^{-1} indicative of asymmetrical $-COO$. This is found in pure alginate spectra but clearly absent from that of PEO, thus confirming the presence of alginate in that fibre.

Fibres from PEO–PAA blends (Fig. 3b) also gave spectra indicating the presence of both polymers and the interactions that occurred during the formation of the blends. A carbonyl peak occurring approximately around 1702 cm^{-1} is typical for pure PAA compounds as confirmed in the spectrum shown. The spectrum for the PEO–PAA blend also shows this carbonyl peak, though with diminished intensity. The intensity of the peak reflects the relatively small proportion of PAA in the blend. There is a slight shift in peak, specifically at 1735 cm^{-1} confirming a complex formation. This shift has been explained by disruption of intramolecular hydrogen bonding in PAA that must occur to make way for interaction with the PEO, and hence a confirmation of some self-associated PAA–PAA hydrogen bonds being replaced by PAA–PEO hydrogen bonds [31].

Finally, determining the presence or otherwise of CMC in the PEO–CMC blends was done by assessing the spectrum of pure CMC compound. A strong peak around 1600 cm^{-1} (Fig. 3c) points to a carboxylate ion $-COO$, which is typical of
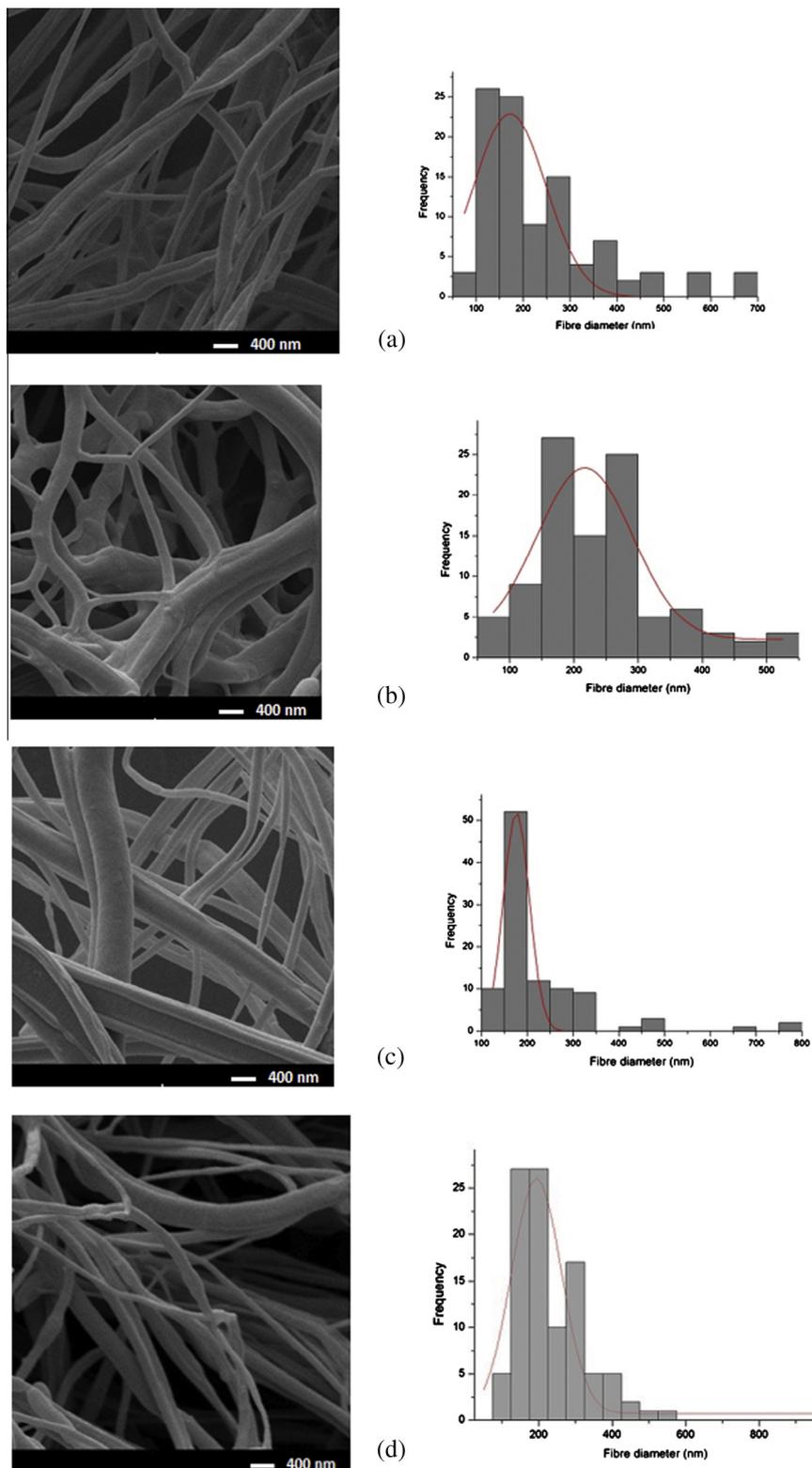
Fig. 1. (a–d) Scanning electron micrographs and size distributions of fibre batches produced from (a) 15% w/w PEO and blends incorporating 75 ml of 15 wt% w/w of PEO and 25 ml of (b) 5% w/w alginate (c) 5% w/w polyacrylic acid and (d) 4% w/w carboxymethylcellulose for any given 100 ml of solution. A gyration speed of 24,000 rpm and working pressure of 0.15 MPa was used.
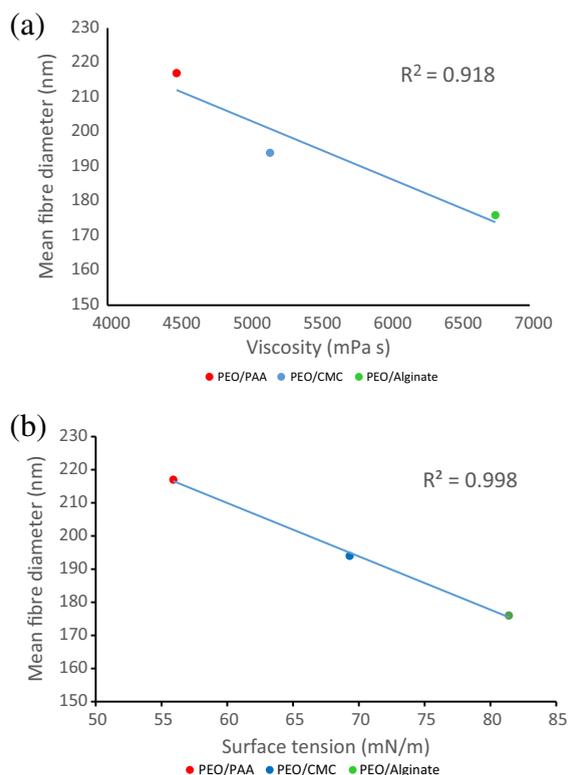
Fig. 2. Correlation between blends (a) viscosity and (b) surface tension and fibre diameter. Fibres were produced from blends incorporating 75 ml of 15 wt% w/w of PEO and 25 ml of (b) 5% w/w alginate (c) 5% w/w polyacrylic acid and (d) 4% w/w carboxymethylcellulose for any given 100 ml of solution.

carboxymethyl cellulose. In the PEO–CMC blend, all characteristic peaks of PEO are seen and in addition, a significant, though diminished peak representative of the carboxylate in CMC. This confirms the presence of CMC in the blend, with the reduction in peak intensity likely to be due to interactions between the carboxylate group from CMC and ether groups from the PEO to ensure miscibility during the blend formation.

Variable temperature FTIR was carried out to examine if the batches of fibres reacted differently to heat exposure (Fig. 4). The blends largely containing PEO were scanned over increasing temperatures up to 80 °C, well above the melting point of PEO. It was observed that the characteristic peak at 843 cm^{-1} indicating a –CH2–CO rocking/stretching for PEO was gradually diminishing with increasing temperature. A more interesting observation was the emergence of new peaks around 663 cm^{-1} for all fibres made from the polymer blends. There was no significant peak in this region for the fibres made up of PEO alone. This observation also confirms the presence of additional material in the fibres from polymer blends. A peak in this region could signify the presence of several functional groups, notably alkyl-halides, specifically C–Br groups, thioether C–S stretch and alkyne C–H groups [32]. Further analysis may be required to identify these new peaks seen upon exposure to heat beyond the melting point of PEO but the current objective of a variable temperature of FTIR was to find out if the fibres from the blends reacted differently compared to those from only PEO in the presence of heat.

3.5. Mucoadhesion and drug encapsulation

Measuring the force required to detach preparations of polymer from mucosa surfaces or environments mimicking mucosa has often been considered useful in predicting the extent of mucoadhesion capabilities of the materials [33–35]. A relationship between viscosities or gel strengths of polymer–mucin systems have also been found to correlate strongly with mucoadhesion properties of polymers [25,36,37]. All these are useful for accurately measuring such quantitative values for predicting the mucoadhesive potential of polymeric systems. Mucoadhesive studies to date, however remains an area with widely differing reports on the same materials by different research groups and hence it is worth noting its limitations and need for considering each case within a context of methodology, experimental conditions and case specific interpretation of results [15,38]. In this context, an approach based on measuring the force corresponding to the gel strength of polymer/mucin system in a simulated vaginal fluid condition was carried out. This force was taken as a quantitative function of the extent and strength of interaction between the polymeric structures and mucosa surface. Baseline studies analysing the interactions between mucin and polymer materials in similar proportions as those used in blends for producing fibres were carried out. The forces measured were compared to another set where the powdered mixtures were replaced with
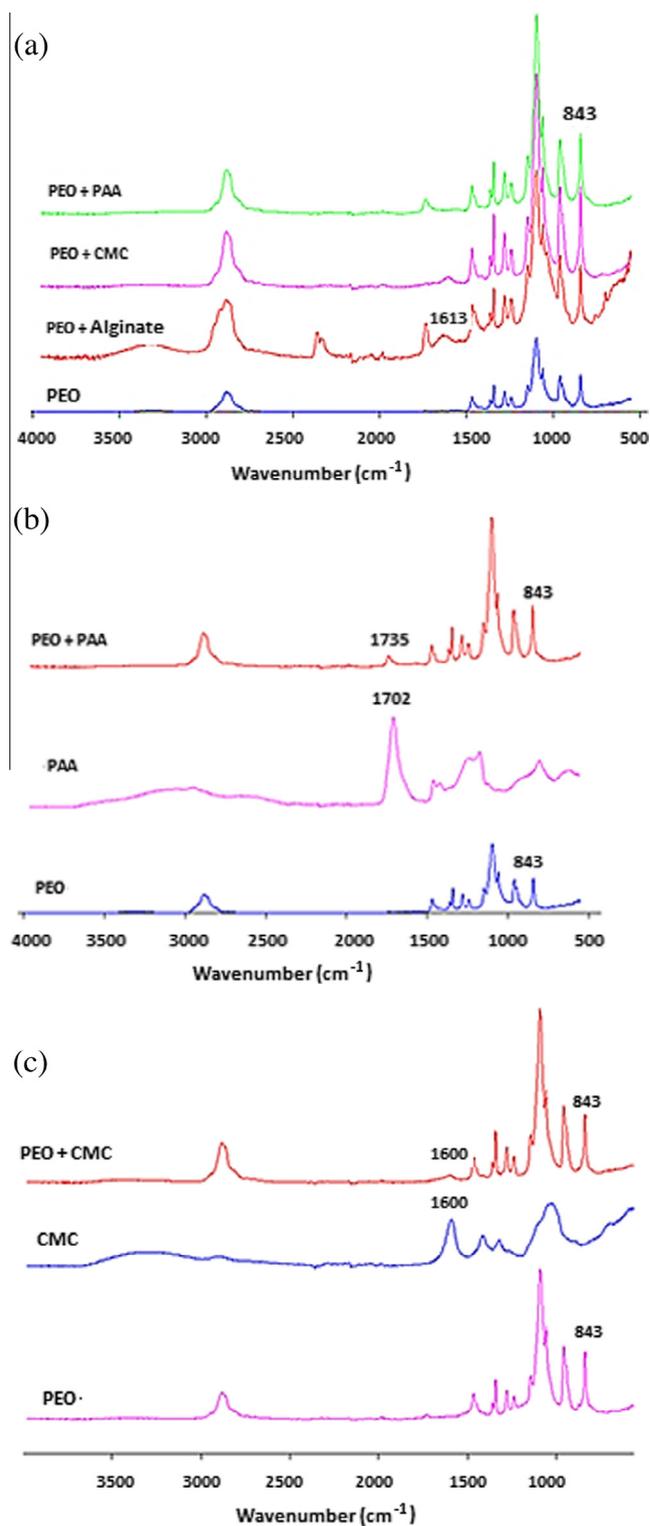
Fig. 3. FTIR spectra (a) comparing PEO fibres to those of PEO/Alginate, PEO/CMC and PEO/PAA blends, (b) comparing PEO/PAA fibres to PAA and PEO polymers and (c) comparing PEO/CMC fibres to CMC and PEO polymers.
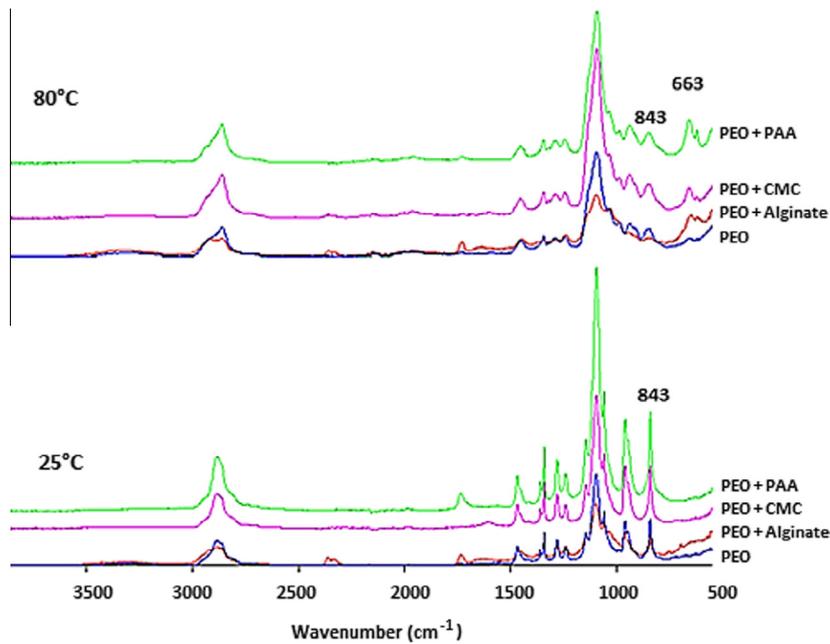
Fig. 4. Variable temperature FTIR spectra of fibres from PEO and blends containing Alginate, CMC and PEO.

fibres. The aim was to see if transforming materials into fibre structures improved their mucoadhesive prospects. As seen in Fig. 5, an increase in mucoadhesive potential was observed in all fibre/mucin systems confirming better adhesive properties after transforming the powders into fibres. A significant increase in surface area of the fibres, providing more sites for interaction with the mucin must have contributed to the increase in forces behind the gel strength.

Specifically, the mucoadhesive potential for the polymer powders occurred in the order PEO/Alginate > PEO/CMC > PEO > PEO/PAA implying that Alginate and CMC in blends with PEO in the powder forms are more likely to offer strong contact by adhesion on mucosa surfaces. Unlike the trend seen with the powder mixtures, fibres with PEO alone showed the weakest interaction with mucin while the remaining batches made of blends demonstrated higher mucoadhesive potential thus confirming the value of producing fibres from blends of different polymers.

A number of characteristics, including polymer chain entanglement related to molecular weight [39] and net charge distribution, whether cationic, neutral or anionic [20] have often been used to explain the mucoadhesive behaviour of polymers. However, none of these characteristics appear in certain terms to explain the trend seen considering the fact that all three polymers mixed with PEO to form blends are anionic with average molecular weight in the order PAA > CMC > Alginate, quite different from the trend CMC > PAA > Alginate seen in Fig. 5. A possible intervention of a carboxylic group in mucoadhesion through hydrogen bonding may be helpful for explaining the trend seen from the mucoadhesive studies [40] since all three polymers in question yield different amounts of carboxylic acid groups. The blend containing carboxymethylcellulose appear to offer the best mucoadhesive prospects throughout the study.
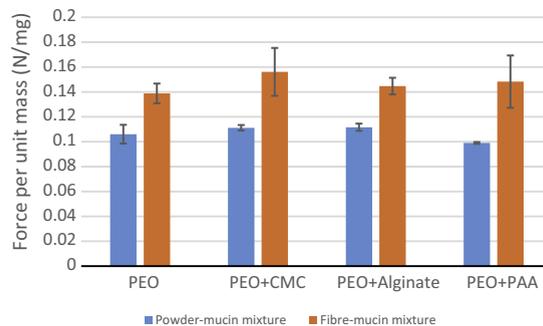

Fig. 5. The effect of transformation from polymer powders to fibres on potential mucoadhesive properties. Higher adhesion capabilities were measured in fibre systems from all batches. Fibres were produced from blends incorporating 75 ml of 15 wt% w/w of PEO and 25 ml of 5% w/w alginate, 5% w/w polyacrylic acid and 4% w/w carboxymethylcellulose for any given 100 ml of solution.
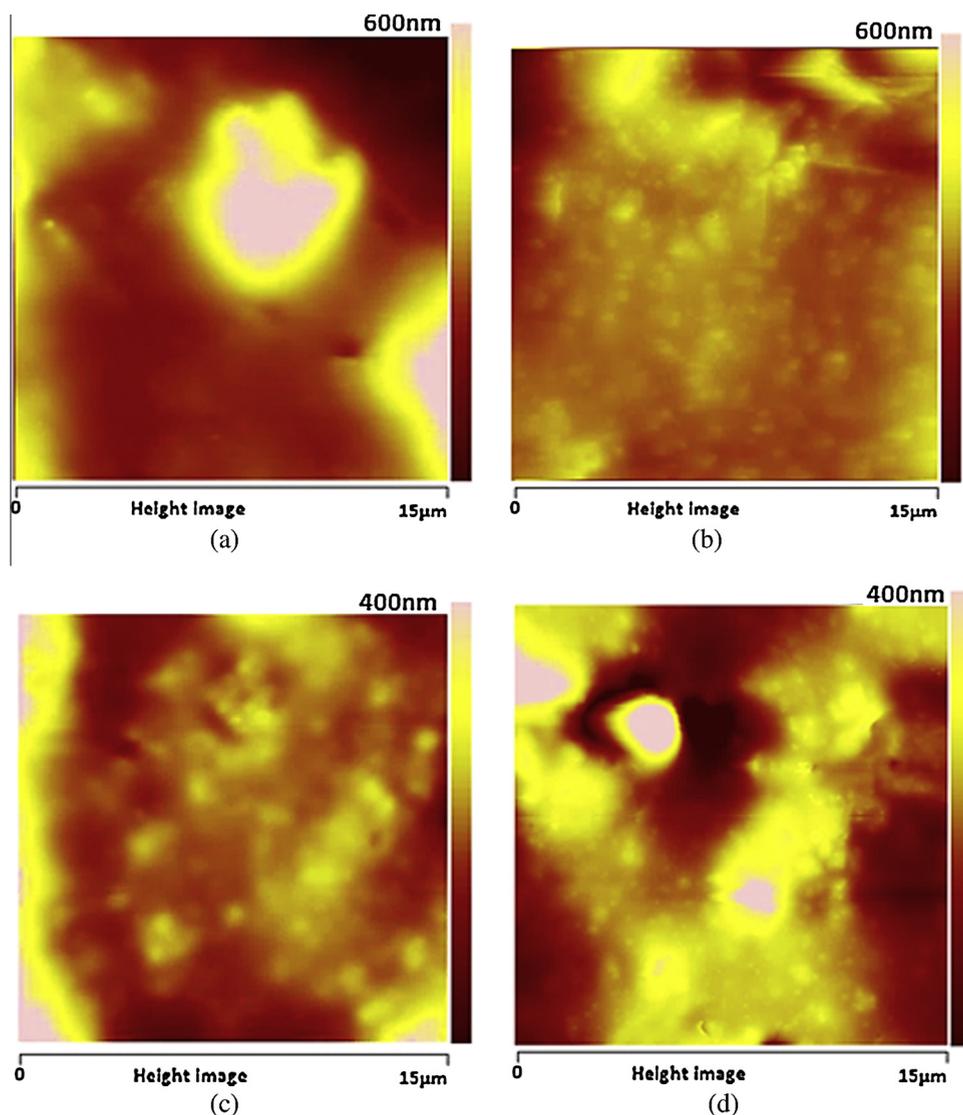
Fig. 6. (a–d) Atomic force micrographs from residual films resulting from fibres/mucin mixtures in simulated vaginal fluid. Fibres produced are from blends incorporating 75 ml of 15 wt% w/w of PEO and 25 ml of (b) 5% w/w alginate (c) 5% w/w polyacrylic acid and (d) 4% w/w carboxymethylcellulose for any given 100 ml of solution.

Several theories have been used to explain how mucoadhesion occurs. Two of these theories [41,42], the wetting theory including hydration also largely considered a prerequisite for facilitating hydrogen bonding for molecular interaction and the diffusion theory where interpenetration of polymer chains across an adhesive interface must have occurred prior to gel formation between the fibres and mucin.

Dried residues resulting from fibre/mucin mixtures were analysed for surface roughness to determine the extent of dissolution of the fibres within the simulated vaginal environment to establish if any correlation exists between this and mucoadhesion. Extent of dissolution of fibres should offer some helpful insights of the level of hydration occurring prior to mucoadhesion. Typically, if complete dissolution of fibres occurred, then the residual film upon drying should be smooth, hence an analysis of the surface roughness. The sum of all areas on the height images (Fig. 6) above 300 nm were calculated with the help of ImageJ software and taken to be a function of roughness of the film surfaces. Out of a total image area 225 μm^2, PEO/Alginate, PEO, PEO/CMC, PEO/PAA had 133 μm^2, 114 μm^2, 104 μm^2 and 83 μm^2, respectively, being above 300 nm. This observation correlates with the mucoadhesion measurements carried out earlier where PEO and PEO/Alginate were shown to have left a rougher residual film and recorded lower forces of adhesion while blends containing CMC and PAA which yielded a smoother residual film demonstrated higher adhesive forces. It is likely the extent of dissolution of the fibres in the mucin – simulated vaginal fluid mixture may actually have played a role in hydration prior to mucoadhesion and hence the trend seen.

A detailed study on drug encapsulation is beyond the scope of this work. However, it should be noted that work in progress is attempting the efficient encapsulation and release of progesterone in nanofibres generated from PEO and PEO–CMC blends by pressurised gyration. Progesterone was chosen because it is one of drugs routinely delivered vaginally [43]. Moreover in recent times, there has been revived interest in progesterone as lead choice for managing preterm labour in women considered at risk [44]. In terms of effect of drug and choice of drug that could be used in this system, as with most nanofibre encapsulation of drugs, the solubility of the drug in the polymer solution is crucial. Hence the choice of drug should be decided in relation to miscibility with the polymer solution. A drug affecting the solution properties of the carrier polymer can impact the outcome of the fibre diameter distribution and encapsulated drug in the fibres.

4. Conclusions

Polymeric structures combining the qualities of high surface area and mucoadhesive capabilities for drug delivery through mucosa surfaces have been produced using blends made from polyethyleneoxide and the mucoadhesive polymers carboxymethylcellulose, sodium alginate and polyacrylic acid. The structures in the form of fibres with size distribution from less than 100 nm upwards have been produces by a simple but efficient method of pressurised gyration. Scanning electron microscopy has confirmed that these fibres are well defined, uniformly cylindrical throughout their lengths and of appreciably high structural integrity. Fourier transform infrared analyses have established the presence of the mucoadhesive polymers and their complexes in the respective fibres, thus confirming pressurised gyration to be useful for the production of fibres incorporating different polymers. A texture analyser and atomic force microscopy were used to study the extent of interaction of these fibres with mucin in a simulated vaginal fluid to help predict their mucoadhesion potential and it was observed that the blend containing carboxymethylcellulose consistently demonstrated the best prospect of mucoadhesion.

Acknowledgements

Appendix A. Supplementary material

Supplementary data associated with this article can be found, in the online version, at http://dx.doi.org/10.1016/j.eurpolymj.2015.07.006.

References

[1] J.-H. He, Electrospun Nanofibres and their Applications, Smithers Rapra Technology, 2008.
[2] L. Cronje, B. Klumperman, Modified electrospun polymer nanofibers as affinity membranes: the effect of pre-spinning modification versus post-spinning modification, Eur. Polym. J. 49 (12) (2013) 3814–3824.
[3] A. Aluigi et al, Structure and properties of keratin/PEO blend nanofibres, Eur. Polym. J. 44 (8) (2008) 2465–2475.
[4] O. Jirsák, T. Dao, Production properties and end-uses of nanofibres, in Nanotechnology in Construction 3. 2009, Springer. p. 95–99.
[5] A. Frenot, M.W. Henriksson, P. Walkenström, Electrospinning of cellulose-based nanofibers, J. Appl. Polym. Sci. 103 (3) (2007) 1473–1482.
[6] N. Bhardwaj, S.C. Kundu, Electrospinning: a fascinating fiber fabrication technique, Biotechnol. Adv. 28 (3) (2010) 325–347.
[7] H.L. Schreuder-Gibson, P. Gibson, Applications of electrospun nanofibers in current and future materials, in: ACS Symposium Series, ACS Publications, 2006.
[8] C. Luo et al, Electrospinning versus fibre production methods: from specifics to technological convergence, Chem. Soc. Rev. 41 (13) (2012) 4708–4735.
[9] R. Qi et al, Electrospun poly (lactic-co-glycolic acid)/halloysite nanotube composite nanofibers for drug encapsulation and sustained release, J. Mater. Chem. 20 (47) (2010) 10622–10629.
[10] M. Beck-Broichsitter et al, Novel 'Nano in Nano' composites for sustained drug delivery: biodegradable nanoparticles encapsulated into nanofiber non-wovens, Macromol. Biosci. 10 (12) (2010) 1527–1535.
[11] A.F. Wei et al, Biodegradable electrospun fibers containing the compound antihypertensive drugs, Adv. Mater. Res. 332 (2011) 1218–1222.
[12] A. Aluigi et al, Adsorption of copper(II) ions by keratin/PA6 blend nanofibres, Eur. Polym. J. 47 (9) (2011) 1756–1764.
[13] Y. Lu et al, Parameter study and characterization for polyacrylonitrile nanofibers fabricated via centrifugal spinning process, Eur. Polym. J. 49 (12) (2013) 3834–3845.
[14] S. Mahalingam, M. Edirisinghe, Forming of polymer nanofibers by a pressurised gyration process, Macromol. Rapid Commun. 34 (14) (2013) 1134–1139.
[15] V. Grabovac, D. Guggi, A. Bernkop-Schnürch, Comparison of the mucoadhesive properties of various polymers, Adv. Drug Deliv. Rev. 57 (11) (2005) 1713–1723.
[16] S. Padron et al, Production and characterization of hybrid BEH-PPV/PEO conjugated polymer nanofibers by forcespinning™, J. Appl. Polym. Sci. 125 (5) (2012) 3610–3616.
[17] Z.-M. Huang et al, A review on polymer nanofibers by electrospinning and their applications in nanocomposites, Compos. Sci. Technol. 63 (15) (2003) 2223–2253.
[18] Q.P. Pham, U. Sharma, A.G. Mikos, Electrospinning of polymeric nanofibers for tissue engineering applications: a review, Tissue Eng. 12 (5) (2006) 1197–1211.
[19] J. Smart, I. Kellaway, H. Worthington, An in-vitro investigation of mucosa-adhesive materials for use in controlled drug delivery, J. Pharm. Pharmacol. 36 (5) (1984) 295–299.
[20] V.V. Khutoryanskiy, Advances in mucoadhesion and mucoadhesive polymers, Macromol. Biosci. 11 (6) (2011) 748–764.
[21] C. Valenta, The use of mucoadhesive polymers in vaginal delivery, Adv. Drug Deliv. Rev. 57 (11) (2005) 1692–1712.

[22] R. Shaikh et al, Mucoadhesive drug delivery systems, J. Pharm. Bioallied Sci. 3 (1) (2011).
[23] R.R. de Araújo Pereira, M.L. Bruschi, Vaginal mucoadhesive drug delivery systems, Drug Dev. Ind. Pharm. 38 (6) (2012) 643–652.
[24] M.R. Marques, R. Loebenberg, M. Almukainzi, Simulated biological fluids with possible application in dissolution testing, Dissolution Technol. 18 (3) (2011) 15–28.
[25] S. Tamburic, D.Q. Craig, A comparison of different in vitro methods for measuring mucoadhesive performance, Eur. J. Pharm. Biopharm. 44 (2) (1997) 159–167.
[26] S.L. Shenoy et al, Role of chain entanglements on fiber formation during electrospinning of polymer solutions: good solvent, non-specific polymer–polymer interaction limit, Polymer 46 (10) (2005) 3372–3384.
[27] T. Caykara et al, Poly (ethylene oxide) and its blends with sodium alginate, Polymer 46 (24) (2005) 10750–10757.
[28] S. Padron et al, Experimental study of nanofiber production through forcespinning, J. Appl. Phys. 113 (2) (2013) 024318.
[29] A. Sionkowska et al, Molecular interactions in collagen and chitosan blends, Biomaterials 25 (5) (2004) 795–801.
[30] Z. Zhang et al, Rheology and morphology of phase-separating polymer blends, Macromolecules 34 (5) (2001) 1416–1429.
[31] C. Alkan et al, Complexing blends of polyacrylic acid-polyethylene glycol and poly (ethylene-co-acrylic acid)-polyethylene glycol as shape stabilized phase change materials, Energy Convers. Manag. 64 (2012) 364–370.
[32] J. Coates, Interpretation of infrared spectra, a practical approach, Encyclopedia of Analytical Chemistry, Wiley, 2006.
[33] C.-M. Lehr et al, In vitro evaluation of mucoadhesive properties of chitosan and some other natural polymers, Int. J. Pharm. 78 (1) (1992) 43–48.
[34] C. Eouani et al, In-vitro comparative study of buccal mucoadhesive performance of different polymeric films, Eur. J. Pharm. Biopharm. 52 (1) (2001) 45–55.
[35] C. Tang et al, New superporous hydrogels composites based on aqueous Carbopol® solution (SPHCcs): synthesis, characterization and in vitro bioadhesive force studies, Eur. Polym. J. 41 (3) (2005) 557–562.
[36] M.K. Marschütz, A. Bernkop-Schnürch, Thiolated polymers: self-crosslinking properties of thiolated 450 kDa poly (acrylic acid) and their influence on mucoadhesion, Eur. J. Pharm. Sci. 15 (4) (2002) 387–394.
[37] C. Caramella et al, Rheological and tensile tests for the assessment of polymer–mucin interactions, Eur. J. Pharm. Biopharm. 40 (4) (1994) 213–217.
[38] H. Hägerström, K. Edsman, Limitations of the rheological mucoadhesion method: the effect of the choice of conditions and the rheological synergism parameter, Eur. J. Pharm. Sci. 18 (5) (2003) 349–357.
[39] N. Thirawong et al, Mucoadhesive properties of various pectins on gastrointestinal mucosa: an in vitro evaluation using texture analyzer, Eur. J. Pharm. Biopharm. 67 (1) (2007) 132–140.
[40] H. Park, J.R. Robinson, Mechanisms of mucoadhesion of poly (acrylic acid) hydrogels, Pharm. Res. 4 (6) (1987) 457–464.
[41] J.D. Smart, The basics and underlying mechanisms of mucoadhesion, Adv. Drug Deliv. Rev. 57 (11) (2005) 1556–1568.
[42] S.-H.S. Leung, J.R. Robinson, Polymer structure features contributing to mucoadhesion. II., J. Controll. Release 12 (3) (1990) 187–194.
[43] Joint Formulary Committee, British National Formulary, 65th ed., BMJ Group and Pharmaceutical Press, London, 2013.
[44] F. Fuchs, F. Audibert, M.-V. Senat, Progesterone and preterm delivery: back to the future?, Gynecol Obstet. Fertil. 42 (2) (2014) 112–122.